

Network Design for Accurate Vehicle Localization

José A. del Peral-Rosado ¹, Member, IEEE, Gonzalo Seco-Granados ², Senior Member, IEEE, Sunwoo Kim ³, Senior Member, IEEE, and José A. López-Salcedo ⁴, Senior Member, IEEE

Abstract—Network-based localization plays a key role on the introduction of emerging road applications, such as connected autonomous driving. These applications demand unprecedented precise, reliable and secure positioning, with localization requirements below 1 m. This stringent demand is pushing for the use of road-side units (RSUs) from fifth generation and vehicular networks for accurate vehicle localization. However, these networks are not typically designed for positioning but for data communication purposes, which follow a different paradigm for the network deployment and operation. This paper provides design guidelines on dedicated network deployments with the aim of achieving accurate vehicle-to-infrastructure positioning in road scenarios. First, the network layout or site placement is assessed with a geometrical metric. Then, the minimum density of RSUs along the road is bounded with line-of-sight probability models for urban street and highway scenarios. Finally, the Cramér–Rao bound for joint time-of-arrival (ToA) and angle-of-arrival (AoA) localization is used to maximize the distance between RSUs along the road, by exploiting multi-antenna deployments. According to the simulation results, the network sites are recommended to be located at alternate sides of the road, with a maximum distance between RSUs of 40 and 230 m for urban and rural environments, respectively. Following these design guidelines, there is also the need to exploit antenna arrays to combine uplink ToA and AoA estimates, in order to ensure a vehicle location accuracy below one meter on the 95% of the cases. The use of eight antenna elements at the RSUs is found to reduce nearly one and a half times the minimum network density in highway localization deployments.

Index Terms—5G, vehicle localization, CRB, ToA, AoA.

I. INTRODUCTION

CONNECTED autonomous driving leads the evolution of road transportation with emerging applications, such as collision avoidance, automated overtake or high-density platooning [1]. These applications are envisaged to significantly improve road safety and traffic management, but their implementation poses challenging requirements on localization and

Manuscript received September 14, 2018; revised January 7, 2019; accepted February 20, 2019. Date of publication March 20, 2019; date of current version May 28, 2019. This work was supported in part by the Spanish Ministry of Science, Innovation and Universities under Project TEC2017-89925-R and in part by the MSIT (Ministry of Science, ICT), Korea, under the ITRC (Information Technology Research Center) support program (IITP-2019-2017-0-01637) supervised by the IITP (Institute for Information & Communications Technology Promotion). The review of this paper was coordinated by Prof. C. Liu. (*Corresponding author: José A. del Peral-Rosado.*)

J. A. del Peral-Rosado, G. Seco-Granados, and J. A. López-Salcedo are with the Department of Telecommunications and Systems Engineering, Universitat Autònoma de Barcelona, Cerdanyola del Vallès 08193, Spain (e-mail: JoseAntonio.DelPeral@uab.cat; Gonzalo.Seco@uab.cat; Jose.Salcedo@uab.cat).

S. Kim is with the Department of Electronic Engineering, Hanyang University, Seoul 04763, South Korea (e-mail: remero@hanyang.ac.kr).

Digital Object Identifier 10.1109/TVT.2019.2906485

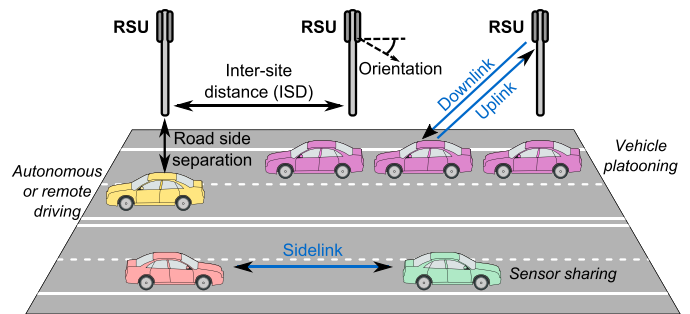


Fig. 1. V2X communications interfaces and emerging vehicular applications.

communications. The automotive sector demands precise and reliable vehicle localization with a positioning accuracy below one meter, and high connectivity between vehicles and the road infrastructure with a low latency [1]. To cope with these challenges, advanced localization systems are based on the fusion of vehicle's on-board sensors [2], such as Global Navigation Satellite Systems (GNSS), radars, cameras and odometers, and vehicle-to-everything (V2X) communications are adopted in vehicular networks to disseminate assistance information, such as the location of the vehicles in the road. As it is shown in Fig. 1, the V2X air interfaces are based on the downlink and uplink vehicle-to-infrastructure (V2I) transmissions by using dedicated base stations (BSs) or road-side units (RSUs) placed along the road, and on the sidelink vehicle-to-vehicle (V2V) transmissions. Furthermore, the robustness of vehicle-based localization is expected to be enhanced with map-aided positioning techniques [3]. However, this conventional approach does not exploit the potential positioning capabilities of V2X networks.

A. State-of-the-Art on V2X Positioning

The use of V2X communications for positioning purposes is mainly studied in the literature with cooperative algorithms. As it is discussed in [4], V2X transmissions are considered as signals of opportunity to obtain measurements for vehicle localization. These signal measurements can be based on the signal strength, ranging, angle or Doppler shift estimates, and their positioning performance is typically evaluated with the theoretical limits defined by the Cramér–Rao Bound (CRB). Considering the implementation issues and performance limitations of these methods, dedicated RSU deployments are usually required in order to achieve sub-meter localization accuracy. This performance level is shown in [5] to be achieved with the cooperative use of angle-of-arrival (AoA) measurements from V2V and V2I

transmissions. Lane-accurate positioning can also be obtained by combining round-trip time (RTT) and AoA estimates from a single and cooperative BS located at a traffic intersection, as it is studied in [6] and it is further assessed in [7] by including the impact of inter-cell interference. Nonetheless, these opportunistic positioning solutions assume full cooperation between vehicles and the network with proprietary solutions, which may not be feasible in commercial deployments with different operators and vehicle manufacturers. Thus, V2X-based localization still needs to be standardized.

B. Standardization Constraints and Perspectives

Current vehicular systems are mainly based on the IEEE 802.11p standard [8], and future deployments are expected to also follow the Long Term Evolution (LTE) Advanced Pro specification [9]. However, none of these standards supports V2X cooperative positioning. The main reason is due to the centralized nature of network deployments. First, network operators are reluctant to disseminate information about the network architecture, such as the location of the BSs and their synchronization, which is necessary to compute the vehicle location in a distributed approach [10], especially with time-of-arrival (ToA) techniques. This has led to the predominance of network-based localization approaches in cellular networks, as it is reviewed in [11], where the device position is computed with downlink or uplink measurements in a network server. Second, the deployment of small cells is mainly dedicated to support communications purposes, thus the implementation of dedicated RSUs for positioning needs to be carefully assessed due to the extra infrastructure cost. Last but not least, network-based positioning protocols are based on snapshot algorithms to compute the device location, by using one or few consecutive measurements transferred in a single location message, as in the LTE positioning protocol (LPP) [12]. Thus, the standard protocols do not include a continuous stream of consecutive positioning measurements, as it is typically considered in navigation or tracking algorithms that filter the measurements and vehicle position over time. These considerations need to be taken into account for the proposal of feasible and accurate vehicle location algorithms.

The fifth generation (5G) cellular networks includes disruptive technologies for vehicular positioning [13], such as high carrier frequencies, large bandwidths, large number of antennas, V2V communications and network densification. These technologies have triggered new mechanisms to achieve high-accuracy positioning, such as single-BS localization [14], cooperative algorithms [15], large-bandwidth allocation [16] or deployment of ultra-dense networks [17]. Indeed, current Release 16 of the 5G specification includes a study on new radio (NR) positioning support [18], but it considers relaxed target requirements with respect to high-accuracy positioning, which can be defined by a position accuracy below 1 m for the 95% of the service area, as it is demanded by vehicular use cases in [19]. Furthermore, the assessment of V2I-based localization, as well as V2V and V2X positioning, is left for future study items. This assessment is expected to inherit the positioning mechanisms of

previous standards and to adopt potential new methods. Thus, the optimized design of dedicated network deployments for V2I positioning is envisaged as a key element of network-based vehicle localization.

C. State-of-the-Art on Network Design for Positioning

The deployment of RSUs along the road has been studied in the literature for vehicular communications, such as in [20]. However, the network design for vehicle localization has had a very limited attention. General metrics are derived in [21] and [22] to evaluate the best placement of wireless networks for localization, by considering the quality of the signal measurements and the geometry of the BSs. In ultra-dense networks, the list of detected BSs is optimally used in [23] to achieve accurate positioning based on Voronoi diagrams, but this proximity approach is expected to lack precision in vehicular deployments. Signal strength measurements are not considered neither for precise vehicle localization, due to their high variance and the relatively high grid resolution required in fingerprinting approaches [24], [25]. In contrast, ranging measurements are envisaged for high-accuracy vehicle positioning, because their achievable performance significantly increases with the signal bandwidth, although a tight network synchronization is required. Considering ranging measurements and the CRB, the optimal placement of BSs is studied in [26] and [27], and the optimal selection of BSs for localization is assessed in [28]. Despite the extra infrastructure introduced with antenna arrays, AoA measurements can complement ToA measurements in vehicular network deployments with deficient geometries and limited signal bandwidth. This is the case of inline sensors discussed in [29], similarly to the V2I scenario, where the distance between sensors is maximized. From a geometrical perspective, the optimal placement of RSUs along a straight road is studied for localization in [30], resulting in equi-spaced RSUs at both sides of the road. However, none of these last two contributions consider the propagation channels, where non-line-of-sight (NLoS) conditions significantly degrade the performance of the signal measurements. The propagation conditions are considered in [31] to evaluate the performance limits of inline localization sensors with the CRB, but this study does not minimize the network density of the deployment.

D. Motivation and Objectives

Overall, the optimal network design has been studied using generic frameworks, but the problem has not been tackled with the specific constraints of vehicular scenarios and network standards. Therefore, two main challenges need to be resolved for a feasible implementation of V2I-based localization. First, the minimum network density or maximum distance between equi-spaced RSUs should be found over representative scenarios, in order to fulfill the automotive localization requirements at a minimum infrastructure cost. And second, the need of additional antenna elements at dedicated RSUs should be clarified in terms of enhanced positioning with respect to conventional single-antenna deployments.

The objective of this paper is to shed light on the network site placement and the exploitation of antenna arrays, in order to achieve accurate V2I-based localization, i.e., 95-% sub-meter positioning as required in [19]. For this purpose, two main novel contributions are provided in this paper. First, design guidelines on the minimum network density are provided for 5G and vehicular deployments, by considering the line-of-sight (LoS) propagation conditions. Second, the CRB for joint ToA and AoA localization is used to evaluate network-based snapshot algorithms, in order to assess the potential benefits of antenna arrays in uplink V2I positioning with improved urban and rural deployments. Our study is based on sub-6 GHz multicarrier schemes, but our design methodology can be adopted with other modulations, frequency bands, propagation models or use cases. Indeed, the deployment of dedicated BSs is perfectly suitable to railway scenarios.

The outline of this paper is as follows. The vehicular system model is described in Section II. The CRB for joint ToA and AoA localization is defined in Section III. The proposed network design is presented in Section IV. These design guidelines and the achievable localization performance of vehicular networks are then evaluated and discussed in Section V. Finally, conclusions and future work are drawn in Section VI.

II. VEHICULAR SYSTEM MODEL

Vehicular scenarios are characterized by the deployment of network sites along the road. The main deployments are defined for urban and highway scenarios, as it is specified in the current standards and research projects [32]. Urban scenarios are described by a Manhattan grid of streets with BSs located at each intersection. Highway scenarios are represented by BSs or RSUs deployed at the centre of the road or at the side of the road, with a specific inter-site distance (ISD). In both scenarios, the location of network sites can be defined as $\mathbf{x}_j = [x_j, y_j]^T$ for $j = \{1, 2, \dots, N_{\text{BS}}\}$, where N_{BS} is the number of sites, and the vehicle location is $\mathbf{x} = [x, y]^T$. Thus, the distance between vehicle and the j -th network site is

$$d_j = \|\mathbf{x} - \mathbf{x}_j\|. \quad (1)$$

This two-dimensional (2D) coordinate system is here considered for the vehicle location problem, since the target requirements are defined in the lane and longitudinal axis. Nonetheless, the system model can be easily adapted to three-dimensional (3D) coordinates for other use cases, such as unmanned aerial vehicles (UAVs).

The current 5G and vehicular communications are based on multicarrier orthogonal frequency-division multiplexing (OFDM) modulations, due to their flexibility to allocate network resources in time and frequency. This flexibility helps to dedicate pilot subcarriers, in order to obtain uplink or downlink signal measurements between vehicle and network sites. Following current standard approaches, network-based localization is then implemented by fusing these measurements in a network server that computes the vehicle location. In this study, only uplink V2I

transmissions are considered to obtain ranging and angle measurements at independent occasions for snapshot-based vehicle localization.

The fundamental issues on the network design for vehicle localization mainly depend on the geometry between network elements, the propagation conditions, and the positioning algorithm selected. To provide network design guidelines, this work considers the following assumptions on the system model:

- The channel model is characterized by distance-dependent LoS conditions. Since NLoS measurements do not improve the localization accuracy without a priori knowledge of the NLoS bias [33], this work focuses on the measurements from the set of network sites in LoS conditions, i.e., \mathcal{N}_{L} , with a total of LoS network sites defined as $|\mathcal{N}_{\text{L}}| \leq N_{\text{BS}}$. This can be achieved by using an NLoS identification technique from those widely studied in the literature, such as in [34], [35], [36] and the references therein, which are able to detect and discard the NLoS measurements. As a result, the network site placement is here determined by the location method and the geometry between vehicle and BSs or RSUs in LoS conditions. This approach is considered to evaluate the minimum network density required to fulfill the localization requirements with snapshot positioning.
- Uplink pilot signals are transmitted from the vehicle to the network sites, and the sites perform the signal measurements over additive white Gaussian noise (AWGN).
- The antenna of each network site is formed by a uniform linear array (ULA) of M elements with known orientation, which has a separation between elements equal to d_a , while the vehicle has an omnidirectional antenna. Each network site has two sector of antenna arrays oriented to each direction of the road.
- The network sites are uniformly distributed along the road with a fixed ISD, and they can be placed at one edge or both edges of the road. This equi-spaced approach maximizes the localization coverage on the road. An example of one-sided RSUs deployment is shown in Fig. 1.
- Network sites are synchronized to a certain reference time, and the vehicle has its own clock. Thus, there is a clock offset between transmitter and receiver. The receiver BSs need to be tightly synchronized below 10 ns [37] to perform accurate ToA measurements. This can be achieved with GNSS-equipped BSs or advanced synchronization protocols [37].
- Signal measurements are obtained by each network site in the far-field region, being the signals received as planar waves at each antenna element. A total of N_m consecutive measurements per snapshot occasion are used to compute the vehicle position at a network server.
- The signal bandwidth B is sufficiently low with respect to the carrier frequency f_c , i.e., narrowband assumption, to consider constant path losses over the transmitted band.

According to the previous assumptions, the vector of uplink received signals at the antenna array of the j -th LoS network site in \mathcal{N}_{L} is defined as

$$\mathbf{y}_j(t) = h_j \cdot \mathbf{a}_j(\phi_j, \alpha_j) \cdot s(t - \tau_j) + \mathbf{w}_j(t), \quad (2)$$

where t is the receiver time instant, h_j is the channel coefficient of the direct path, \mathbf{a}_j is the antenna steering vector, ϕ_j is the angle between vehicle and site, α_j is the orientation of the antenna array at the network site, $s(t)$ is the uplink pilot signal, $\tau_j = d_j/c + \delta t$ is the propagation delay, being c the speed of light and δt the vehicle clock offset, and $\mathbf{w}_j(t)$ is a zero-mean complex Gaussian noise vector with two-sided power spectral density N_0 . The antenna steering vector of the ULA is defined as

$$\mathbf{a}_j(\phi_j, \alpha_j) \doteq \left[1, e^{j \frac{2\pi \cdot f_c \cdot d_a \cdot \cos(\phi_j - \alpha_j)}{c}}, \dots, e^{j \frac{2\pi \cdot (M-1) \cdot f_c \cdot d_a \cdot \cos(\phi_j - \alpha_j)}{c}} \right]^T, \quad (3)$$

where

$$\phi_j = \tan^{-1} \left(\frac{y - y_j}{x - x_j} \right). \quad (4)$$

The uplink multicarrier OFDM signal is written as

$$s(t) = \sqrt{\frac{2C}{N}} \sum_{n \in \mathcal{N}_{sc}} b_n \cdot p_n \cdot \exp \left(j \frac{2\pi n t}{T} \right), \quad (5)$$

where C is the signal power, N is the total number of subcarriers, \mathcal{N}_{sc} is the subset of active subcarrier indexes, b_n is the complex-valued symbol transmitted at the n -th subcarrier, the relative power weight p_n^2 is constrained by $\sum_n p_n^2 = N$, and T is the OFDM symbol period, which is defined by the subcarrier spacing F_{sc} as $T = 1/F_{sc}$. The signal-to-noise ratio (SNR) at j -th network site is finally defined (in dB) as

$$\text{SNR}_j = P_{\max} - L_j - \text{SF}_j - N_0 - \text{NF} - 10 \cdot \log_{10}(B), \quad (6)$$

where P_{\max} is the maximum transmit power, L_j are the macroscopic path losses, SF_j is the shadow fading, NF is the receiver noise figure, and $B = N \cdot F_{sc}$ is the signal bandwidth. The macroscopic path losses are computed as

$$L_j = \max(\text{PL}(d_j) - A(\phi_j, \alpha_j) - G_{\text{rx}}, \text{MCL}), \quad (7)$$

where $\text{PL}(d_j)$ follows a path loss model (for LoS conditions) defined in [38], the antenna pattern is [39]

$$A(\phi_j, \alpha_j) = G_{\text{TX}} - \min \left(12 \left(\frac{\phi_j - \alpha_j}{\phi_{3\text{dB}}} \right)^2, A_{\min} \right), \quad (8)$$

being G_{TX} the antenna gain, $\phi_{3\text{dB}}$ the 3-dB beamwidth and A_{\min} the minimum attenuation, G_{rx} is the receiver antenna gain, and MCL is the minimum coupling loss (MCL).

III. JOINT TOA/AOA CRAMÉR–RAO BOUND

The CRB for joint ToA and AoA localization provides a lower bound on the achievable positioning accuracy, when obtaining time-delay and angle measurements with antenna arrays at different network sites. Thus, this lower bound can be used to determine the network design guidelines for accurate vehicle localization. This section first describes the general formulation of the joint ToA/AoA CRB, and then the network design criteria is presented by using this CRB formulation.

A. General Formulation

The position accuracy is defined by the root-mean-square error (RMSE) of the position estimate $\hat{\mathbf{x}}$, and it is bounded by the square root of the joint CRB of the position \mathbf{x} with ranging and angle measurements as

$$\varepsilon_{\mathbf{x}, \text{Joint}} = \sqrt{\mathbb{E}[\|\hat{\mathbf{x}} - \mathbf{x}\|^2]} \geq \sqrt{\text{tr}\{\mathbf{CRB}_{\text{Joint}}(\mathbf{x})\}}, \quad (9)$$

where $\mathbb{E}[\cdot]$ is the expectation and $\text{tr}\{\cdot\}$ is the trace operator. The position estimation is based on a vector of unknown parameters formed by

$$\boldsymbol{\theta} = [\boldsymbol{\tau}, \boldsymbol{\phi}, \delta t, \mathbf{h}]^T, \quad (10)$$

where $\boldsymbol{\tau} = [\tau_1, \tau_2, \dots, \tau_{|\mathcal{N}_L|}]^T$ is the vector of time delays, $\boldsymbol{\phi} = [\phi_1, \phi_2, \dots, \phi_{|\mathcal{N}_L|}]^T$ is the vector of angles, and $\mathbf{h} = [h_1, h_2, \dots, h_{|\mathcal{N}_L|}]^T$ is the vector of channel coefficients from the $|\mathcal{N}_L|$ sites considered for positioning. As it is derived in [31], the CRB can be computed with the equivalent Fisher information matrix (EFIM) by assuming \mathbf{h} as nuisance parameters, i.e.,

$$\mathbf{CRB}_{\text{Joint}}(\mathbf{x}) = [\mathbf{J}_{\text{Joint}}^{-1}(\mathbf{x}, \delta t, \mathbf{h})]_{1:2,1:2}. \quad (11)$$

The EFIM for the joint ToA and AoA positioning is

$$\mathbf{J}_{\text{Joint}}(\mathbf{x}, \delta t, \mathbf{h}) = \mathbf{J}_{\text{ToA}}(\mathbf{x}, \delta t, \mathbf{h}) + \mathbf{J}_{\text{AoA}}(\mathbf{x}, \delta t, \mathbf{h}), \quad (12)$$

where the joint EFIM is decoupled into the EFIM for ToA positioning $\mathbf{J}_{\text{ToA}}(\mathbf{x}, \delta t, \mathbf{h})$ and the EFIM for AoA positioning $\mathbf{J}_{\text{AoA}}(\mathbf{x}, \delta t, \mathbf{h})$, which is similarly derived in [40] for joint ToA/AoA with known clock offset. The EFIM for ToA positioning is defined as [31]

$$\mathbf{J}_{\text{ToA}}(\mathbf{x}, \delta t, \mathbf{h}) = \mathbf{H}_{\text{ToA}}^T \mathbf{C}_{\text{ToA}}^{-1} \mathbf{H}_{\text{ToA}}, \quad (13)$$

where \mathbf{H}_{ToA} is a $|\mathcal{N}_L| \times 3$ matrix defined as

$$[\mathbf{H}_{\text{ToA}}]_{j,1:3} = \begin{bmatrix} \frac{x-x_j}{d_j} & \frac{y-y_j}{d_j} & 1 \end{bmatrix}, \quad (14)$$

and \mathbf{C}_{ToA} is a $|\mathcal{N}_L| \times |\mathcal{N}_L|$ square matrix expressed as

$$\mathbf{C}_{\text{ToA}} = \text{diag} \left(\sigma_{1,\text{ToA}}^2, \sigma_{2,\text{ToA}}^2, \dots, \sigma_{|\mathcal{N}_L|,\text{ToA}}^2 \right) \quad (15)$$

with

$$\sigma_{j,\text{ToA}}^2 = \frac{c^2}{8\pi^2 \cdot N_m \cdot M \cdot \text{SNR}_j \cdot \sum_{n \in \mathcal{N}_{sc}} p_n^2 \cdot n^2}. \quad (16)$$

The EFIM for AoA positioning is expressed as [31]

$$\mathbf{J}_{\text{AoA}}(\mathbf{x}, \delta t, \mathbf{h}) = \mathbf{H}_{\text{AoA}}^T \mathbf{C}_{\text{AoA}}^{-1} \mathbf{H}_{\text{AoA}}, \quad (17)$$

where \mathbf{H}_{AoA} is a $|\mathcal{N}_L| \times 3$ matrix defined as

$$[\mathbf{H}_{\text{AoA}}]_{j,1:3} = \begin{bmatrix} -\frac{y-y_j}{d_j^2} & \frac{x-x_j}{d_j^2} & 0 \end{bmatrix}, \quad (18)$$

and \mathbf{C}_{AoA} is a $|\mathcal{N}_L| \times |\mathcal{N}_L|$ square matrix written as

$$\mathbf{C}_{\text{AoA}} = \text{diag} \left(\sigma_{1,\text{AoA}}^2, \sigma_{2,\text{AoA}}^2, \dots, \sigma_{|\mathcal{N}_L|,\text{AoA}}^2 \right) \quad (19)$$

with

$$\sigma_{j,\text{AoA}}^2 = \frac{c^2}{8\pi^2 \cdot N_m \cdot M \cdot \text{SNR}_j \cdot f_c^2 \cdot G_{\text{ULA}}(\phi_j, \alpha_j)}, \quad (20)$$

and the squared array aperture function of the ULA is

$$G_{\text{ULA}}(\phi_j, \alpha_j) = \frac{(M^2 - 1) \cdot d_a^2}{12} \cdot \sin^2(\phi_j - \alpha_j). \quad (21)$$

The CRB for ToA positioning, i.e., when using only time-delay measurements, is defined as

$$\text{CRB}_{\text{ToA}}(\mathbf{x}) = [\mathbf{J}_{\text{ToA}}^{-1}(\mathbf{x}, \delta t, \mathbf{h})]_{1:2,1:2}. \quad (22)$$

From (13), the use of multiple antennas is equivalent to the use of multiple measurements in terms of position accuracy with ToA localization, which is written as $\varepsilon_{\mathbf{x}, \text{ToA}} \geq \sqrt{\text{tr}\{\text{CRB}_{\text{ToA}}(\mathbf{x})\}}$. In the case of using only angle measurements, the CRB for AoA positioning is defined as

$$\text{CRB}_{\text{AoA}}(\mathbf{x}) = \left([\mathbf{J}_{\text{AoA}}(\mathbf{x}, \delta t, \mathbf{h})]_{1:2,1:2}\right)^{-1}, \quad (23)$$

and the position accuracy is $\varepsilon_{\mathbf{x}, \text{AoA}} \geq \sqrt{\text{tr}\{\text{CRB}_{\text{AoA}}(\mathbf{x})\}}$. Comparing (13) with (17), d_j and d_a has a higher impact on $\mathbf{J}_{\text{AoA}}(\mathbf{x}, \delta t, \mathbf{h})$ than on $\mathbf{J}_{\text{ToA}}(\mathbf{x}, \delta t, \mathbf{h})$. As a result, the CRB for joint ToA and AoA positioning is mainly dominated by the ToA measurements for high signal bandwidth, while the AoA measurements are certainly more relevant for short distances between vehicle and sites and a high number of antenna elements. Furthermore, the joint ToA and AoA approach is able to compute the vehicle location with one site less than the ToA approach with unknown clock offset, as well as it relaxes the geometric problem with more than two BSs or RSUs. This can be of special interest for vehicular scenarios, where few BSs or RSUs (with a deficient location geometry) can be connected with the vehicle.

Considering equal $\sigma_{j, \text{ToA}}^2$ and $\sigma_{j, \text{AoA}}^2$ for each LoS network site, the quality of the location geometry can be measured with the horizontal dilution of precision (HDOP), which is here defined for the ToA case as

$$\text{HDOP}_{\text{ToA}}(\mathbf{x}) = \sqrt{\text{tr}\left\{\left(\mathbf{H}_{\text{ToA}}^T \mathbf{H}_{\text{ToA}}\right)^{-1}\right\}}. \quad (24)$$

A reduced value of $\text{HDOP}_{\text{ToA}}(\mathbf{x})$ (e.g. below 2) corresponds to an excellent location geometry, while a large HDOP (e.g. above 10) indicates a poor geometry for positioning.

B. Network Design Criteria

The provision of accurate vehicle location services leads to the consideration of network design criteria based on the vehicle positioning accuracy and availability. In this sense, the aim of the network design is to minimize the network density while fulfilling the positioning requirements with snapshot algorithms. To do so, the joint ToA/AoA CRB is here used to determine the fulfillment of the design criteria.

Considering the dedicated deployment of equi-spaced RSUs along a straight road as in Fig. 1, the densification of sites for a road segment is mainly defined by the ISD. Thus, the minimization of the network density is equivalent to the maximization of the ISD. This ISD maximization is limited by the provision of a certain positioning accuracy and availability for the possible vehicle positions under the coverage area. Then, this optimization

problem can be formulated as

$$\begin{aligned} \text{ISD}_{\text{max}} &= \max \text{ISD}, \\ \text{s.t. } &P_{\text{acc}}(\varepsilon_{\mathbf{x}} \leq \varepsilon_{\text{thr}} \mid \text{ISD}, \mathbf{x}) \geq P_{\text{thr}} \forall \mathbf{x} \in S, \end{aligned} \quad (25)$$

where $S = \{\mathbf{x} \in \mathbb{R}^2 \mid |x| < x_{\text{max}}, |y| < y_{\text{max}}\}$ is the service coverage area, being x_{max} and y_{max} the maximum coverage in the x - and y -coordinates, respectively, $\varepsilon_{\mathbf{x}}$ is the vehicle position accuracy, P_{acc} is the probability of position solutions that fulfill the positioning accuracy required ε_{thr} given a certain ISD, and P_{thr} is the positioning availability or probability of position fix required. For this optimization, the best possible accuracy is considered, i.e., $\varepsilon_{\mathbf{x}} = \sqrt{\text{tr}\{\text{CRB}_{\text{ToA}}(\mathbf{x})\}}$ for ToA positioning and $\varepsilon_{\mathbf{x}} = \sqrt{\text{tr}\{\text{CRB}_{\text{Joint}}(\mathbf{x})\}}$ for joint ToA and AoA positioning. In case there are not enough LoS measurements to solve the CRB, the position accuracy is set to infinity. Since a distance-dependent LoS probability is assumed in the system model, the ISD maximization results in a combinatorial problem. Thus, the maximum ISD, ISD_{max} , is here resolved through Monte-Carlo simulations by adopting the proposed design guidelines described as in the next section.

IV. PROPOSED NETWORK DESIGN

This section proposes a novel network design approach to deploy dedicated RSUs for accurate vehicle localization. First, the network design parameters are introduced, and then network design guidelines are presented to solve the maximization problem described in (25).

A. Design Parameters

The main design parameters to tailor a communications network for accurate vehicle localization are here summarized.

1) *Inter-Site Distance*: The ISD is the separation between BSs or RSUs along the road. This parameter defines the network density, which has a relevant impact on the cost of the deployed infrastructure.

2) *Road Side Separation*: The road side separation d_r is the lateral distance between vehicle and BS or RSU. This is also an important parameter to consider for positioning, because it defines (with the ISD) the geometric problem.

3) *Number of Positioning Sites*: The solution of the positioning problem requires a minimum number of independent measurements from different sites. For instance, the joint ToA and AoA localization only requires two BSs or RSUs, thanks to the combination of ranging and angle measurements.

4) *Antenna Array Configuration*: The deployment of antenna arrays at each network site allows the computation of AoA measurements. The resolution of these angle measurements depends on the number of antenna elements, the separation between elements and the orientation of the array. The two-sectorial site with directional antennas is the preferred configuration for conventional RSUs [41], and dedicated deployments may include antenna arrays with two or four elements at each sector site. Thus, the standard deviation of AoA estimates is above 1.8 degrees, as it can be computed with (20) for an ULA

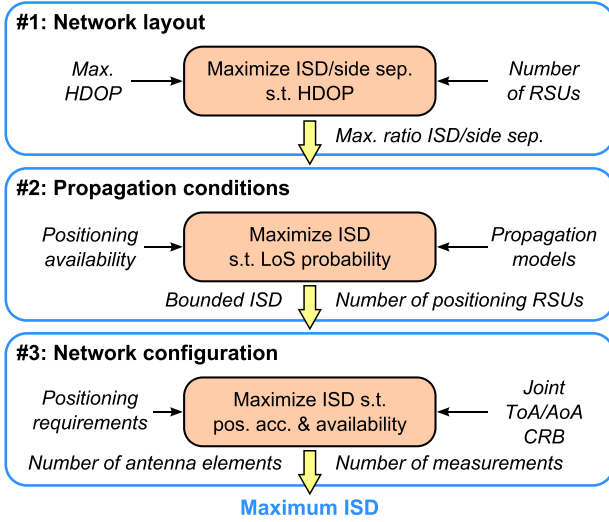


Fig. 2. Proposed network design approach for accurate vehicle localization.

of four antenna elements spaced half-wavelength, SNR of 10 dB and an incident angle of 90 degrees.

5) *Network Resources*: Dedicated positioning resources are necessary for accurate localization in vehicular networks. First, wideband pilot signals result in a low variance on the ToA measurements. Then, the network coordination avoids signal interference of time and frequency resources. These pilot signals are transmitted in positioning occasions, whose periodicity can be configured by the network operator as a trade-off of the positioning accuracy and the pilot overhead [42]. For instance, the LTE standard specifies the positioning reference signal (PRS) with a minimum periodicity equal to 160 ms and 10 ms for wideband and narrowband transmissions, respectively [43]. Finally, a positioning protocol is used to exchange assistance, measurement and positioning messages, which also fulfills security purposes.

B. Design Guidelines

The proposed network design is based on three main guidelines to feasibly resolve the optimization problem in (25), by fulfilling the positioning requirements with snapshot methods and a minimum network density or maximum ISD. These guidelines tackle the optimization from the most general to the most specific design parameters. The general diagram of the proposed approach is shown in Fig. 2. As it can be seen, the problem solution of the maximum ISD is bounded at each step by designing the main network parameters. These design guidelines are further described next.

1) *Network Layout*: The network layout determines the location of the RSUs with respect to the road. Since the dedicated deployment is considered to be based on equi-spaced RSUs, the main design parameters of the network layout are the ISD, road side separation and number of positioning sites. Indeed, the first two parameters can be coupled with a ratio defined as $\eta = \text{ISD}/d_r$. This ratio certainly determines the positioning capabilities of a certain deployment pattern, e.g. equi-spaced RSUs deployed at one side or at both sides, from a geometrical perspective. These positioning capabilities are then measured with

$\text{HDOP}_{\text{ToA}}(\mathbf{x})$, defined in (24). In general terms, a ratio η close to one results in a low HDOP due to the high angular diversity between vehicle and RSUs. However, since the RSUs are located close to the road side, a low ratio η increases the network density. Therefore, as a first guideline, the ratio between ISD and road side separation is maximized subject to a maximum HDOP, which is formulated as

$$\eta_{\max} = \max \eta, \quad \text{s.t. } \text{HDOP}_{\text{ToA}}(\mathbf{x}) \leq \text{HDOP}_{\max} \quad \forall \mathbf{x} \in S, \quad (26)$$

where HDOP_{\max} is the maximum HDOP pre-defined. This maximization is resolved numerically for a certain number of positioning sites, resulting in the design of a maximum ratio η_{\max} . In addition, the maximum number of sites can be considered for this computation, since the available RSUs for positioning are expected to be reduced due to the propagation conditions, as it is discussed next.

2) *Propagation Conditions*: The propagation conditions determine the number of available positioning sites, which are those sites in LoS conditions. Since distance-dependent propagation models are considered, the propagation conditions vary depending on the vehicle and RSU locations. That is, the LoS probability is determined by the distance d_j , i.e., $P_{\text{LoS}}(d_j)$, and the SNR at j -th site is determined by the distance d_j and angle ϕ_j that (together with orientation α_j) characterize the macroscopic path losses defined in (7). One can notice that the range of distances and angles between the vehicle and RSUs is mainly bounded by the ISD and road side separation. For example, given a vehicle close to the first RSU, i.e., $x = x_1$, the distances and angles are defined as

$$d_j = \sqrt{d_r^2 + (|j| - 1)^2 \cdot \text{ISD}^2}, \quad (27)$$

$$\phi_j = \tan^{-1}(d_r / ((|j| - 1) \cdot \text{ISD})). \quad (28)$$

Considering the maximum ratio η_{\max} obtained in the previous guideline, the ISD can be maximized to ensure the availability of a certain number of positioning sites, for a certain road side separation. Thus, the second guideline is formulated as

$$\begin{aligned} \text{ISD}'_{\max} &= \max \text{ISD}, \\ \text{s.t. } &P_{\text{pos}}(|\mathcal{N}_L| \geq N_{\text{pos}} \mid \text{ISD}, \mathbf{x}) \geq \\ &P_{\text{thr}} \quad \forall \mathbf{x} \in S, \end{aligned} \quad (29)$$

where P_{pos} is the probability that the number of RSUs in LoS conditions is above the minimum number of links N_{pos} to compute the position solution. This maximization problem is also computed numerically, since it depends on the propagation models. Furthermore, these models can include additional impairments not considered in this work, such as the inclusion of NLoS misdetections in the LoS probability or inter-cell interferences in the SNR model. Thus, this guideline helps to design the number of positioning sites and to bound the ISD. Still, notice that ISD'_{\max} differs from the maximum ISD obtained in (25), because the positioning accuracy requirement is not yet fulfilled.

3) *Network Configuration*: The network configuration is optimized in this last guideline of the proposed network design. The

antenna array configuration and the network resources are finally optimized to solve the ISD maximization problem in (25). Once the previous guidelines are considered, the main design parameters to be tailored with the ISD maximization are the number of antenna elements M and the number of consecutive measurements N_m . As it is shown in Section III-A, both parameters improve the positioning accuracy, but in addition, the number of antenna elements decrease the minimum number of sites needed for positioning, from $N_{\text{pos}} = 3$ (for only ToA positioning) to $N_{\text{pos}} = 2$ (for joint ToA and AoA positioning). Thus, the fulfillment of the positioning accuracy and availability finally drives the design of the maximum ISD or minimum network density.

V. RESULTS AND DISCUSSION

This section evaluates the proposed network design for accurate vehicle localization in urban and highway dedicated sub-6 GHz deployments. The positioning requirements are defined to achieve 95-% sub-meter positioning with snapshot algorithms, i.e., $\varepsilon_{\text{thr}} = 1$ m and $P_{\text{thr}} = 0.95$. Each design guideline is discussed with simulation results to achieve the optimal site placement and configuration. First, the ToA localization problem is assessed for single-antenna deployments with conventional (i.e., data communication) network parameters, in order to discuss the geometrical constraints of vehicular scenarios. Then, the impact of the propagation conditions is evaluated to bound the ISD optimization. Finally, the impact and achievable performance of the joint ToA and AoA localization is computed with respect to the stand-alone ToA localization, in order to solve the ISD maximization problem and to highlight the potential benefits that angular measurements can bring for positioning purposes.

The numerical evaluations of this section are obtained for urban and highway scenarios with V2I communications, where BSs or RSUs are periodically located with a certain ISD and road side separation. The coordinated transmission of positioning pilots are assumed for a network of six BSs or RSUs, in order to avoid inter-cell interference. For the evaluation, the OFDM physical layer is based on a signal bandwidth of 10 MHz, such as the 802.11p standard, and 64 contiguous pilot subcarriers are allocated per symbol. The vehicle localization is based on one uplink ToA and AoA measurement (i.e., $N_m = 1$) from at least the two closest BSs or RSUs, in order to characterize the performance of snapshot positioning algorithms. The simulation parameters are summarized in Table I. Despite these specific parameters, the guidelines discussed in this work can be extended to other vehicular scenarios with similar network topologies.

A. Conventional Network Deployments

Conventional network deployments along highways are based on BSs located every 500 or 1000 meters and between 10 to 35 meters away from the side of the road or at the center of the road. Dedicated vehicular deployments may have a high density of RSUs along roads with an ISD of 100 or 200 meters for suburban scenarios, and along streets with an ISD around 50 meters for urban scenarios. These deployments are characterized by two-sectorial towers oriented at both directions of the road, as it

TABLE I
SIMULATION PARAMETERS OF THE V2I SCENARIO

$B = 10$ MHz	Site ant. height: $h_{\text{BS}} = 10$ m
$f_c = 5.9$ GHz	Veh. ant. height: $h_{\text{veh}} = 1.5$ m
$F_{\text{sc}} = 156.25$ kHz	# of ant. sectors = 2
$N = 64$ subcarriers	$N_m = 1$ measurement
$n = \{0, 1, \dots, 63\} - 31.5$	$\alpha_j = \tan^{-1}(2d_r/\text{ISD})$
$p^2(n) = 1 \forall n$	$d_a = c/(2f_c)$
$P_{\text{max}} = 23$ dBm	$\phi_{3\text{dB}} = 32^\circ$
$G_{\text{TX}} = 3$ dBi	$A_m = 30$ dB
NF = 9 dB	$G_{\text{RX}} = 8$ dBi
SF _j = 15 dB	MCL = 70 dB
$N_0 \approx -174$ dBm/Hz	$\mathbf{x} = [x, 0]$ m

can be seen in Fig. 1. The quality of their location geometry is here assessed based on the first design guideline, by considering a uniform deployment.

Let us first characterize two generic deployments along a straight road depending on ISD and d_r , by assuming the vehicle location $\mathbf{x} = [x, 0]$. First, the network sites are periodically located at one side of the road, i.e., $\mathbf{x}_j = [k \cdot \text{ISD}, d_r]^T$ with $k = j - \lceil N_{\text{BS}}/2 \rceil$. Second, the network sites are located at alternate sides of the road, i.e., $\mathbf{x}_j = [k \cdot \text{ISD}, d_r]^T$ for $\{2k : k \in \mathbb{Z}\}$ and $\mathbf{x}_j = [k \cdot \text{ISD}, -d_r]^T$ for $\{2k - 1 : k \in \mathbb{Z}\}$, where d_r and d_r' define each side separation. These side separations are related by an asymmetry coefficient γ , as $\gamma = d_r'/d_r$, which is equal to one when the side separation is the same at both sides of the road. The geometrical constraints of these one-sided and two-sided deployments are now assessed with the HDOP defined in (24). This metric is computed at vehicle locations along the x axis, for network deployments of N_{BS} sites characterized by the ratio η . In general terms, the minimum HDOP is found for a vehicle location close to a network site, and the maximum HDOP is found for a vehicle location at a mid distance between the two closest sites. As it is shown in Fig. 3, the two-sided deployments have a better location geometry (i.e., lower HDOP) than the one-sided deployment, as in [30], due to the improved angle diversity of the measurements. This can be especially seen for $N_{\text{BS}} = 3$ and $\eta = 9$, where a two-sided HDOP of five significantly improves the one-sided HDOP of ten. Furthermore, one-sided deployments need to increase the network density and number of sites in order to achieve the same HDOP as two-sided deployments. For instance, the one-sided HDOP of five requires a deployment with $N_{\text{BS}} = 4$ and $\eta = 5$ or with $N_{\text{BS}} = 5$ and $\eta = 6$. For two-sided deployments, the HDOP does not vary for $N_{\text{BS}} \geq 4$, and an increase of the asymmetry coefficient γ has a very slight improvement on the HDOP. As an outcome of this design guideline, two-sided deployments are recommended for a low number of network sites, such as three or four BSs, in order to ensure a good trilateration geometry, i.e., a maximum HDOP around or below five. To achieve this good geometry, the ratio between ISD and d_r should be less than ten.

B. Impact of Propagation Conditions

The LoS and NLoS propagation conditions need to be considered, in order to assess the achievable positioning accuracy for

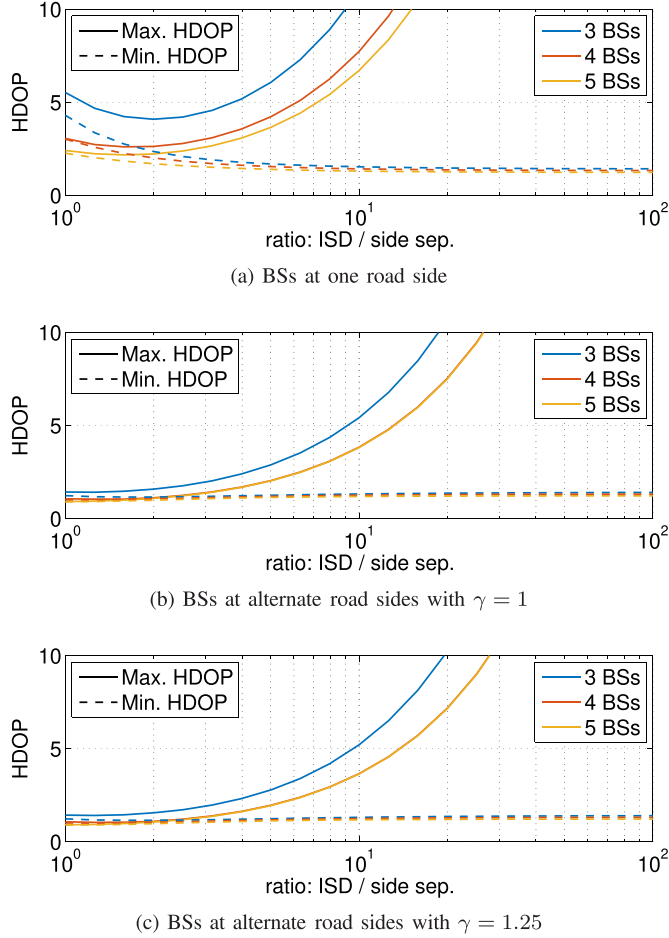


Fig. 3. Maximum and minimum $\text{HDOP}_{\text{ToA}}(\mathbf{x})$ from network sites along a straight road, as function of the ratio between ISD and d_r .

a certain network deployment. These conditions can be characterized by distance-dependent propagation models, such as the WINNER radio channel models [44], which represent indoor and outdoor environments. This section focuses on outdoor urban and rural channel models to study the impact of propagation conditions based on the second design guideline.

Let us consider three standard propagation models defined in [38] for urban micro-cell (i.e., 3D-UMi), urban macro-cell (i.e., 3D-UMa) and rural macro-cell (i.e., 3D-RMa) network deployments. These models are adaptations of the WINNER B1, C2 and D1 models [44], respectively, which can also be adopted for vehicular environments. They define the probability of LoS as function of the distance between network site and vehicle as [38]:

$$P_{\text{LoS,UMi}}(d_j) = \min\left(\frac{18}{d_j}, 1\right) \cdot \left(1 - e^{-\frac{d_j}{36}}\right) + e^{-\frac{d_j}{36}}, \quad (30)$$

$$P_{\text{LoS,UMa}}(d_j) = \min\left(\frac{18}{d_j}, 1\right) \cdot \left(1 - e^{-\frac{d_j}{63}}\right) + e^{-\frac{d_j}{63}}, \quad (31)$$

$$P_{\text{LoS,RMa}}(d_j) = \min\left(e^{-\frac{d_j-10}{1000}}, 1\right). \quad (32)$$

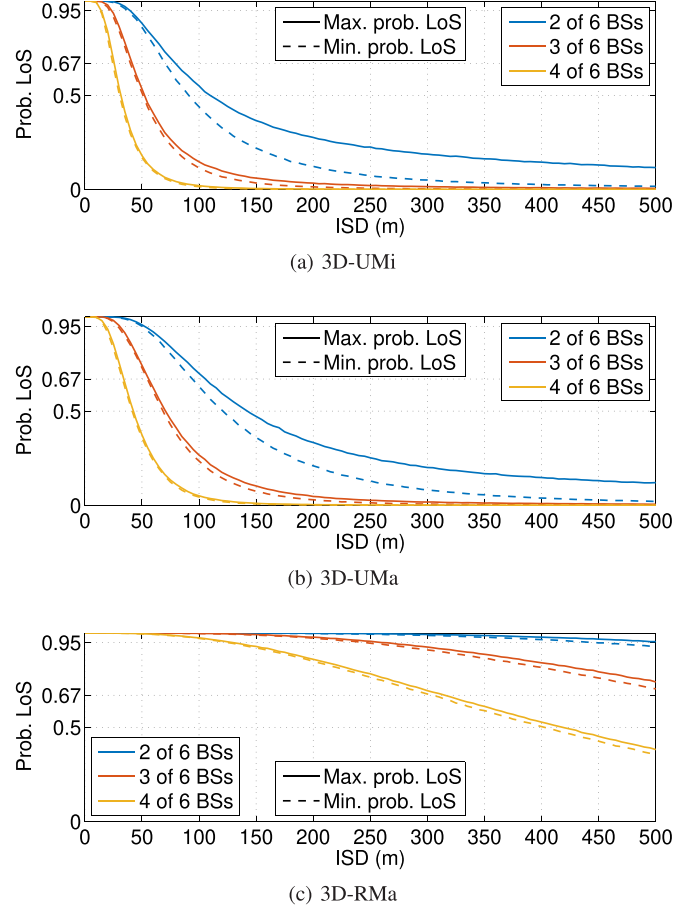


Fig. 4. Maximum and minimum probability of LoS as function of the ISD for outdoor urban and rural channel models, computed with $d_r = 15$ m and 50000 Monte-Carlo simulations.

Notice that the height-dependency factor is omitted in (31), since the vehicle antenna height is set to $h_{\text{veh}} = 1.5$ m.

Now, the second design guideline can be evaluated by considering these LoS probability functions. For this purpose, a maximum number of six coordinated BSs and a road side separation of 15 m are defined, i.e., $N_{\text{BS}} = 6$ and $d_r = 15$ m. Then, the probability P_{pos} or LoS probability of a certain number of BSs is computed as function of the ISD over each channel model, as it is shown in Fig. 4. The maximum LoS probability is found for a vehicle location close to a BS, and the minimum is obtained when the vehicle is in a mid distance between the two closest BSs. Since the 3D-UMi and 3D-UMa models characterize urban areas with predominant NLoS scenarios, the maximum ISD needs to be around 40 and 50 meters, respectively, in order to ensure a LoS probability of 95% for at least two BSs (i.e., $N_{\text{pos}} = 2$). In contrast, the maximum ISD also with $N_{\text{pos}} = 2$ is around ten times more, i.e., 400 and 500 m, for the 3D-RMa model, which represents rural scenarios with a low average building height. As a result, urban deployments require a network density ten times more than rural deployments, in order to ensure a 95-% LoS probability with the same number of positioning sites N_{pos} . Thus, this second guideline helps to design the network density in order to fulfill a certain positioning

TABLE II
URBAN AND RURAL 3GPP PATH LOSS MODELS [38]

3D-UMi/3D-UMa path loss models
$d'_j = \sqrt{d_j^2 + (h_{BS} - h_{veh})^2}$ $d_{BP} = 4 \cdot (h_{BS} - 1) \cdot (h_{veh} - 1) \cdot f_c / c$ $PL(d_j d_j < d_{BP}) = 22 \log_{10}(d'_j) + 28 + 20 \log_{10}(f_c \cdot 10^{-9}),$ $PL(d_j d_j \geq d_{BP}) = 40 \log_{10}(d'_j) + 28 + 20 \log_{10}(f_c \cdot 10^{-9})$ $- 9 \log_{10}(d_{BP}^2 + (h_{BS} - h_{veh})^2).$
3D-RMa path loss models
$d'_j = \sqrt{d_j^2 + (h_{BS} - h_{veh})^2}, h_{av} = 5 \text{ m}$ $d_{BP} = 2\pi \cdot h_{BS} \cdot h_{veh} \cdot f_c / c$ $PL(d_j d_j < d_{BP}) = 20 \log_{10}(40\pi \cdot d'_j \cdot f_c \cdot 10^{-9} / 3)$ $+ \min(0.03h_{av}^{1.72}, 10) \cdot \log_{10}(d'_j)$ $- \min(0.044h_{av}^{1.72}, 14.77)$ $+ 0.002 \log_{10}(h_{av}) \cdot d'_j,$ $PL(d_j d_j \geq d_{BP}) = PL(d_j d_j < d_{BP}) + 40 \log_{10}(d'_j / d_{BP}).$

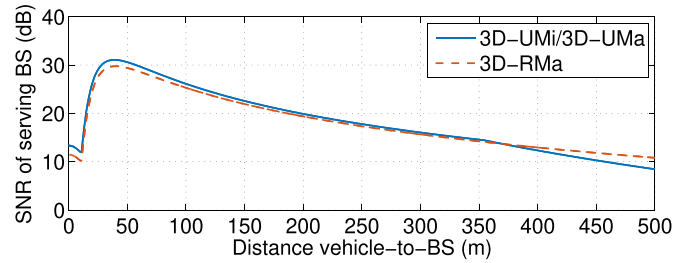
availability in representative scenarios. Furthermore, the results highlight the importance of introducing antenna arrays at each site in order to solve or relax the positioning problem.

As well as the LoS probability, the received signal levels at the network sites need to be assessed, since they determine the quality of the ranging and angle measurements. Thus, the minimum SNR at the different network sites is computed as in (6), by using the path loss models described in Table II. As it is shown in Fig. 5a, the SNR of the serving BS is characterized by the antenna pattern and the path loss models in [38]. Since the antenna array is oriented towards the mid road point between two BSs, i.e., $\alpha_j = \tan^{-1}(2d_r / \text{ISD})$, the SNR is below 15 dB for a vehicle location close to the serving BS. The minimum SNR per BS is also shown in Fig. 5b for the 3D-UMi and 3D-UMa models and in Fig. 5c for the 3D-RMa model. These results show that the minimum SNR of the serving BS is mainly determined by the antenna pattern, while the minimum SNR of the neighbor BSs is mainly characterized by the path losses. Furthermore, when the vehicle is very close to serving cell, the SNR of the serving BS is lower than the SNR of the neighbor BSs, due to the orientation of the two-sectorial antenna.

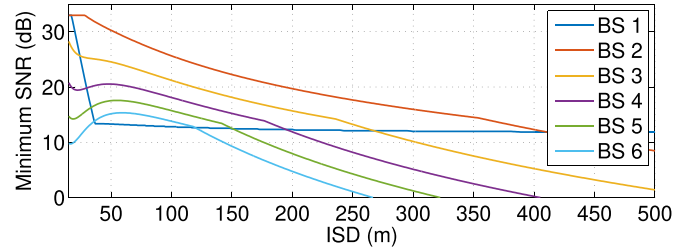
The analysis of the LoS probability and minimum SNR is applicable to one-sided and two-sided deployments, since the distance between vehicle and network sites is practically the same. Thus, the second guideline and the SNR analysis can be used to design and discuss an improved network deployment for accurate vehicle localization, as follows.

C. Improved Network Deployments for Accurate Localization

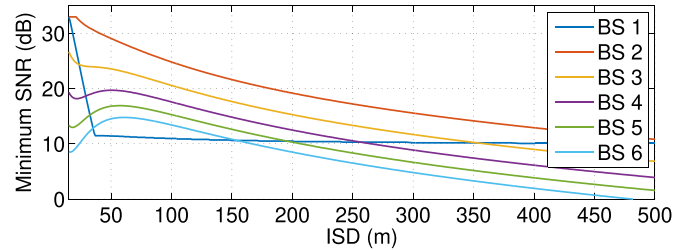
Conventional network deployments have a ratio between ISD and d_r well above ten, which results in a poor HDOP. Improved network deployments can be designed for accurate vehicle localization by reducing the ratio between ISD and d_r to around or below ten, and by locating the RSUs at alternate sides of the road with $\gamma = 1$, as discussed in Section V-A. Still, the achievable localization accuracy of these dedicated deployments needs to be



(a) SNR of serving BS with ISD = 500 m



(b) 3D-UMi and 3D-UMa models



(c) 3D-RMa model

Fig. 5. SNR of the network sites as function of d_j and ISD.

studied. This section assesses improved network deployments designed with the proposed guidelines in urban and rural environments by considering network sites with two, four and eight antenna elements. The signal measurements are assumed to be obtained in LoS and AWGN conditions, where the SNR levels and LoS probabilities are computed with 3D-UMi and 3D-RMa models.

The urban micro-cell deployment requires a high density of RSUs along the straight street. Let us apply the design guidelines 1 and 2 to determine a preliminary network density. As a result, the ISD is defined to 40 meters, in order to achieve a LoS probability around 95% from at least two RSUs (by following the results in Fig. 4), and the road side separation is set to five meters, in order to obtain a good trilateration geometry with a ratio η below 10. Then, the third guideline is applied by using the CRB expressions in (11) and (22) to compute the lower limit on the vehicle location accuracy, which depends on the number and location of the network sites in LoS conditions. As it is shown in Fig. 6a, the achievable location accuracy is well below one meter for both stand-alone and joint approaches, thanks to the high SNR and AWGN conditions of the signal measurements. The sub-meter accuracy is still achieved despite the performance degradation close to the serving RSU (i.e., at $x = k \cdot \text{ISD}$), due to the two-sectorial antenna configuration. The joint ToA and AoA localization is at least two times better than the stand-alone

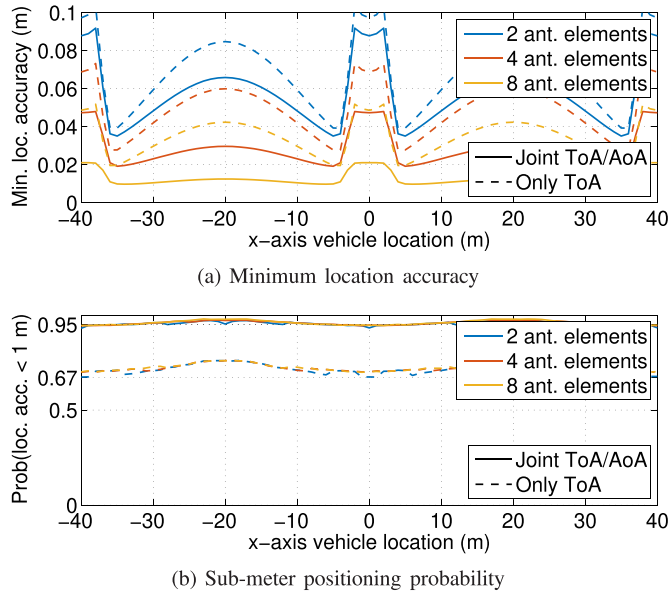


Fig. 6. Localization performance of stand-alone ToA and joint ToA and AoA for ISD = 40 m in AWGN conditions with SNR levels and LoS probabilities computed with the 3D-UMi model, over 50 000 Monte-Carlo simulations.

ToA solution for four or more antenna elements and vehicle locations between network sites (i.e., at $x = k \cdot \text{ISD}/2$). In addition, and as it was expected from guideline 2, the joint approach with four or more antennas is necessary to achieve a 95-% positioning availability (or probability of position fix) with a 2D accuracy below one meter, as it is shown in Fig. 6b. Therefore, these results show a significant benefit on the combination of ranging and angle measurements, and the need to deploy dedicated network sites with antenna arrays of four or more elements to fulfill the high-accuracy and reliable vehicle localization required in urban environments, while minimizing the network density.

The rural macro-cell deployment also needs a relatively high density of network sites along the road. Following the proposed network design as in the previous case, the ISD is set to 200 meters, in order to ensure at least three LoS RSUs for the 95-% of the cases. Due to deployment limitations, the road side separation is set to 15 meters, even if the ratio η is above ten. The achievable location accuracy is then computed with the CRB considering the 3D-RMa model in Fig. 7a. These results show that the stand-alone ToA approach does not ensure a 95-% sub-meter positioning accuracy. In addition, the joint ToA and AoA approach provides a reduced improvement with respect to the urban environment, due to lower SNR levels and higher HDOP in the rural environment. This is due to the higher distances between vehicle and RSUs, which also reduce the AoA contribution as it is expected from (18). Still, the joint approach fulfills the 95-%-availability and sub-meter accuracy requirements for four or more antenna elements, mainly at vehicle locations between RSUs, i.e., $x = k \cdot \text{ISD}/2$. Therefore, this improved sub-6 GHz network deployment is necessary to cope with the positioning accuracy and availability requirements. However, further enhancements are needed at vehicle locations close to

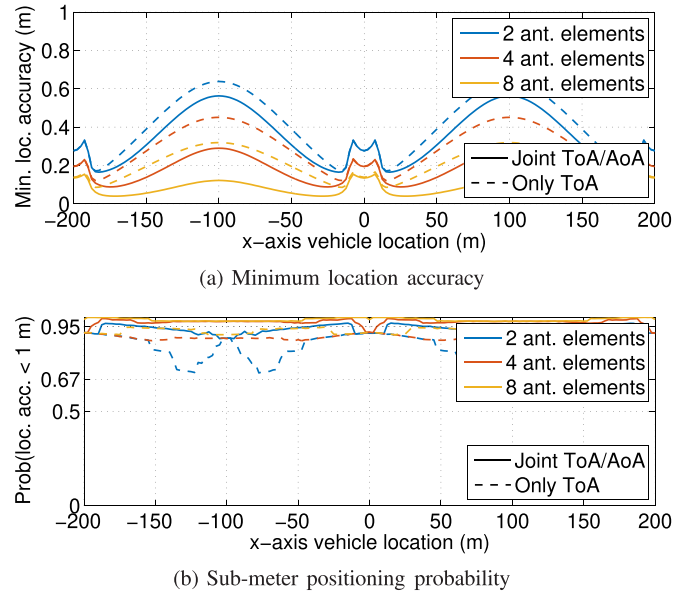


Fig. 7. Localization performance of stand-alone ToA and joint ToA and AoA for ISD = 200 m in AWGN conditions with SNR levels and LoS probabilities computed with the 3D-RMa model, over 50 000 Monte-Carlo simulations.

the serving RSUs, such as by adding another sector or by further optimizing the maximum ISD.

The network design can be optimized in terms of maximum ISD, as it is proposed in the third design guideline, depending on the number of antenna elements and the LoS propagation conditions. This is especially relevant in the rural environment that, despite the predominance of LoS, the achievable positioning accuracy is degraded due to low signal levels and bad geometry. Thus, the 95-% location accuracy is here computed with the CRB expressions as a function of the ISD and the number of antenna elements. This result is obtained for critical vehicle positions, i.e., close to the serving RSU and between RSUs. As it is shown in Fig. 8a, a maximum ISD of around 230 m can be designed by using joint ToA and AoA positioning with eight antennas per site, because this configuration is able to compensate the low SNR levels and high HDOP. Notice that the rest of configurations can only reach a maximum ISD of around 160 m, as it is shown in Fig. 8a, due to the performance limitations when the vehicle is close to the serving RSU (i.e., $x = k \cdot \text{ISD}$). Thus, the eight-antenna design allows to increase the ISD nearly one and a half times with respect to the stand-alone ToA approach. For instance, considering a highway segment of 1.8 km, the number of RSUs necessary to ensure 95-% sub-meter positioning with snapshot algorithms can be reduced from 12 to 8, by exploiting antenna arrays of eight elements to combine ToA and AoA estimates. Therefore, the network density can be minimized by increasing the number of the antenna elements.

Notice the importance of the use of antenna arrays to fulfill the positioning requirements, by considering the effect of multiple antenna elements on the stand-alone ToA positioning. As it is discussed in Section III, an increase on the number of antennas M is equivalent to an increase of the number of consecutive measurements N_m in the ToA positioning. However,

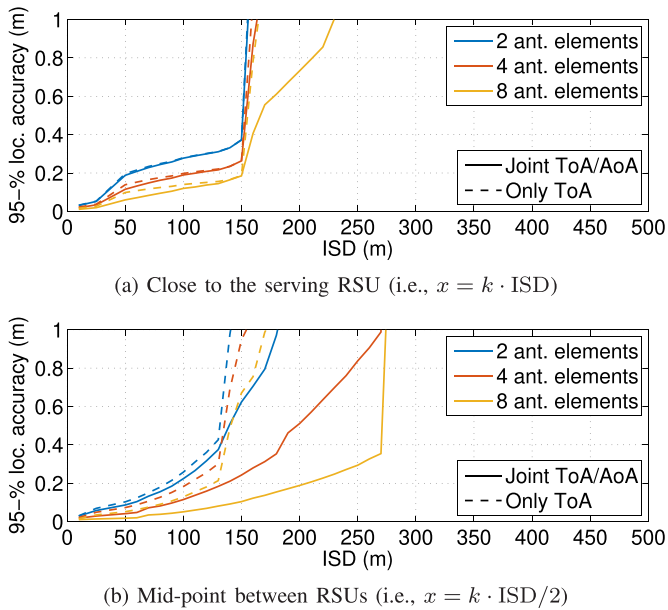


Fig. 8. 95% location accuracy of the joint ToA and AoA localization for vehicle locations at $x = k \cdot \text{ISD}$ and $x = k \cdot \text{ISD}/2$, in AWGN conditions with SNR levels and LoS probabilities computed with the 3D-RMa model over 50000 simulations.

despite the increase of the number of antennas, the ISD is almost not increased with the stand-alone ToA approach, as it is shown in Fig. 8. Instead, the joint ToA/AoA approach succeeds to maximize the ISD with eight antenna elements, thanks to the relaxation of the positioning problem and the improved signal measurements.

The proposed network design has been evaluated in this work based on the joint ToA/AoA CRB, which provides the best position accuracy, in order to assess the minimum network density. Future work is aimed at studying the multipath effect and mitigation of NLoS measurements in the design approach of 5G vehicular networks for high-accuracy positioning.

VI. CONCLUSION

We have studied the network design for accurate vehicle localization, relying on fifth generation (5G) and vehicular communications with dedicated sub-6 GHz deployments. The goal of this design is to minimize the density of road-side units (RSUs) in dedicated networks, while ensuring an achievable positioning accuracy below one meter with a positioning availability of the 95% of the cases. Thus, a novel design approach is proposed to maximize the inter-site distance (ISD) between RSUs, by optimizing the network parameters in terms of network layout, propagation conditions and network configuration. In contrast to conventional deployments, our design guidelines leads to the alternate location of dedicated sites at both sides of the road, with a density bounded by the line-of-sight (LoS) conditions of several links. Then, the uplink positioning accuracy is assessed with the Cramér-Rao bound (CRB) for joint time-of-arrival (ToA) and angle-of-arrival (AoA) localization with unknown clock offset. Using the proposed guidelines with a 10-MHz bandwidth, the simulation results show that urban dedicated deployments require around five times more density

than highway or rural dedicated deployments to fulfill the positioning requirements. The maximum ISD is found to be limited to around 40 m and 230 m in urban and rural environments, respectively. This minimum density requires the use of the joint ToA and AoA approach with eight antenna elements, in order to ensure a two-dimensional (2D) sub-meter accuracy on the 95% of the cases with snapshot algorithms. Therefore, the exploitation of ranging and angle measurements is shown to be necessary to improve the positioning accuracy and availability, as well as to increase nearly one and a half times the maximum ISD, with respect to the use of only ranging measurements. Therefore, the proposed network design is shown to fulfill the positioning requirements with a minimum network densification. Future work aims at further studying the design of 5G networks for accurate vehicle localization considering multipath errors.

REFERENCES

- [1] 5G-PPP, "5G automotive vision," Brussels, Belgium, White Paper, Oct. 2015. [Online]. Available: <https://5g-ppp.eu/wp-content/uploads/2014/02/5G-PPP-White-Paper-on-Automotive-Vertical-Sectors.pdf>
- [2] S. Kuutti, S. Fallah, K. Katsaros, M. Dianati, F. McCullough, and A. Mouzakitis, "A survey of the state-of-the-art localization techniques and their potentials for autonomous vehicle applications," *IEEE Internet Things J.*, vol. 5, no. 2, pp. 829–846, Apr. 2018.
- [3] R. Karlsson and F. Gustafsson, "The future of automotive localization algorithms: Available, reliable, and scalable localization: Anywhere and anytime," *IEEE Signal Process. Mag.*, vol. 34, no. 2, pp. 60–69, Mar. 2017.
- [4] N. Alam and A. G. Dempster, "Cooperative positioning for vehicular networks: Facts and future," *IEEE Trans. Intell. Transp. Syst.*, vol. 14, no. 4, pp. 1708–1717, Dec. 2013.
- [5] A. Fascista, G. Ciccarese, A. Coluccia, and G. Ricci, "Angle of arrival-based cooperative positioning for smart vehicles," *IEEE Trans. Intell. Transp. Syst.*, vol. 19, no. 9, pp. 2880–2892, Sep. 2017.
- [6] H. Kloeden, D. Schwarz, E. M. Biebl, and R. H. Rashofer, "Vehicle localization using cooperative RF-based landmarks," in *Proc. IEEE Intell. Vehicles Symp.*, Jun. 2011, pp. 387–392.
- [7] A. E. Assaad, M. Krug, and G. Fischer, "Vehicle self-localization for advanced driver assistance systems," in *Proc. Workshop Positioning, Navigation Commun.*, Oct. 2016, pp. 1–6.
- [8] J. Gozalvez, M. Sepulcre, and R. Bauza, "IEEE 802.11p vehicle to infrastructure communications in urban environments," *IEEE Commun. Mag.*, vol. 50, no. 5, pp. 176–183, May 2012.
- [9] C. Hoymann *et al.*, "LTE release 14 outlook," *IEEE Commun. Mag.*, vol. 54, no. 6, pp. 44–49, Jun. 2016.
- [10] U. A. Khan, S. Kar, and J. M. F. Moura, "Distributed sensor localization in random environments using minimal number of anchor nodes," *IEEE Trans. Signal Process.*, vol. 57, no. 5, pp. 2000–2016, May 2009.
- [11] J. A. del Peral-Rosado, R. Raulefs, J. A. López-Salcedo, and G. Seco-Granados, "Survey of cellular mobile radio localization methods: From 1G to 5G," *IEEE Commun. Surv. Tuts.*, vol. 20, no. 2, pp. 1124–1148, Apr.–Jun. 2018.
- [12] *LTE Positioning Protocol (LPP)*, Standard 3GPP TS 36.355, Rel. 15, 2018.
- [13] H. Wymeersch, G. Seco-Granados, G. Destino, D. Dardari, and F. Tufvesson, "5G mm-wave positioning for vehicular networks," *IEEE Wireless Commun.*, vol. 24, no. 6, pp. 80–86, Dec. 2017.
- [14] A. Shahmansoori, G. E. Garcia, G. Destino, G. Seco-Granados, and H. Wymeersch, "Position and orientation estimation through millimeter-wave MIMO in 5G systems," *IEEE Trans. Wireless Commun.*, vol. 17, no. 3, pp. 1822–1835, Mar. 2018.
- [15] A. Dammann, R. Raulefs, and S. Zhang, "On prospects of positioning in 5G," in *Proc. IEEE Int. Conf. Commun. Workshop*, Jun. 2015, pp. 1207–1213.
- [16] J. A. del Peral-Rosado, J. A. López-Salcedo, S. Kim, and G. Seco-Granados, "Feasibility study of 5G-based localization for assisted driving," in *Proc. Int. Conf. Localization GNSS*, Jun. 2016, pp. 1–6.
- [17] M. Koivisto *et al.*, "Joint device positioning and clock synchronization in 5G ultra-dense networks," *IEEE Trans. Wireless Commun.*, vol. 16, no. 5, pp. 2866–2881, May 2017.

- [18] *Study on NR Positioning Support*, Standard 3GPP TR 38.855, Rel. 16, 2019.
- [19] *Study on Positioning Use Cases; Stage 1*, Standard 3GPP TR 22.872, Rel. 16, 2018.
- [20] A. B. Reis, S. Sargento, F. Neves, and O. K. Tonguz, "Deploying roadside units in sparse vehicular networks: What really works and what does not," *IEEE Trans. Veh. Technol.*, vol. 63, no. 6, pp. 2794–2806, Jul. 2014.
- [21] S. Mazuelas, R. M. Lorenzo, A. Bahillo, P. Fernandez, J. Prieto, and E. J. Abril, "Topology assessment provided by weighted barycentric parameters in harsh environment wireless location systems," *IEEE Trans. Signal Process.*, vol. 58, no. 7, pp. 3842–3857, Jul. 2010.
- [22] J. Schloemann, H. S. Dhillon, and R. M. Buehrer, "Toward a tractable analysis of localization fundamentals in cellular networks," *IEEE Trans. Wireless Commun.*, vol. 15, no. 3, pp. 1768–1782, Mar. 2016.
- [23] H. Elsawy, W. Dai, M.-S. Alouini, and M. Z. Win, "Base station ordering for emergency call localization in ultra-dense cellular networks," *IEEE Access*, vol. 6, pp. 301–315, 2018.
- [24] A. Alhasanat, B. Sharif, C. Tsimenidis, and J. Neasham, "Efficient RSS-based collaborative localisation in wireless sensor networks," *Int. J. Sensor Netw.*, vol. 22, no. 1, pp. 27–36, 2016.
- [25] A. Al-Qaisi, A. I. Alhasanat, A. Mesleh, B. S. Sharif, C. C. Tsimenidis, and J. A. Neasham, "Quantized lower bounds on grid-based localization algorithm for wireless sensor networks," *Ann. Telecommun.*, vol. 71, no. 5, pp. 239–249, Jun. 2016.
- [26] D. Moreno-Salinas, A. M. Pascoal, and J. Aranda, "Optimal sensor placement for multiple target positioning with range-only measurements in two-dimensional scenarios," *Sensors*, vol. 13, no. 8, pp. 10674–10710, 2013.
- [27] Z. Liu, W. Dai, and M. Z. Win, "Node placement for localization networks," in *Proc. IEEE Int. Conf. Commun.*, 2017, pp. 1–6.
- [28] W. Dai, Y. Shen, and M. Z. Win, "A computational geometry framework for efficient network localization," *IEEE Trans. Inf. Theory*, vol. 64, no. 2, pp. 1317–1339, Feb. 2018.
- [29] S. C. K. Herath and P. N. Pathirana, "Optimal sensor arrangements in angle of arrival (AoA) and range based localization with linear sensor arrays," *Sensors*, vol. 13, no. 9, pp. 12277–12294, 2013.
- [30] R. Zhang, F. Yan, W. Xia, S. Xing, Y. Wu, and L. Shen, "An optimal roadside unit placement method for VANET localization," in *Proc. Global Commun. Conf.*, Dec. 2017, pp. 1–6.
- [31] Y. Han, Y. Shen, X. P. Zhang, M. Z. Win, and H. Meng, "Performance limits and geometric properties of array localization," *IEEE Trans. Inf. Theory*, vol. 62, no. 2, pp. 1054–1075, Feb. 2016.
- [32] METIS project, "D1.4, METIS channel models," Feb. 2015.
- [33] Y. Shen and M. Z. Win, "Fundamental limits of wideband localization—Part I: A general framework," *IEEE Trans. Inf. Theory*, vol. 56, no. 10, pp. 4956–4980, Oct. 2010.
- [34] S. Gezici, H. Kobayashi, and H. V. Poor, "Nonparametric nonlinear-of-sight identification," in *Proc. IEEE Veh. Technol. Conf.*, vol. 4, Oct. 2003–Fall, pp. 2544–2548.
- [35] S. Mazuelas *et al.*, "Prior NLOS measurement correction for positioning in cellular wireless networks," *IEEE Trans. Veh. Technol.*, vol. 58, no. 5, pp. 2585–2591, Jun. 2009.
- [36] S. Marano, W. M. Gifford, H. Wymeersch, and M. Z. Win, "NLOS identification and mitigation for localization based on UWB experimental data," *IEEE J. Sel. Areas Commun.*, vol. 28, no. 7, pp. 1026–1035, Sep. 2010.
- [37] H. Li, L. Han, R. Duan, and G. M. Garner, "Analysis of the synchronization requirements of 5G and corresponding solutions," *IEEE Commun. Stand. Mag.*, vol. 1, no. 1, pp. 52–58, Mar. 2017.
- [38] *Study on 3D Channel Model for LTE*, Standard 3GPP TR 36.873, Rel. 12, 2018.
- [39] *RF System Scenarios*, Standard 3GPP TR 36.942, Rel. 15, 2018.
- [40] S. Jeong, T. K. Sung, K. E. Lee, and J. Kang, "Joint TOA/AOA-based localization in wireless sensor networks," in *Proc. Int. Conf. Signal Process. Commun. Syst.*, Dec. 2014, pp. 1–5.
- [41] V. Shivaldova, A. Paier, D. Smely, and C. F. Mecklenbrucker, "On roadside unit antenna measurements for vehicle-to-infrastructure communications," in *Proc. Int. Symp. Pers., Indoor Mobile Radio Commun.*, Sep. 2012, pp. 1295–1299.
- [42] S. Fischer, "Observed time difference of arrival (OTDOA) positioning in 3GPP LTE," Qualcomm Technologies, San Diego, CA, USA, Tech. Rep., Jul. 2014.
- [43] X. Lin *et al.*, "Positioning for the Internet of Things: A 3GPP perspective," *IEEE Commun. Mag.*, vol. 55, no. 12, pp. 179–185, Dec. 2017.
- [44] IST-WINNER II project deliverable D1.1.2, "WINNER II channel models," Eur. Commission, Brussels, Belgium, Tech. Rep., 2007.



he gave tutorials at IEEE ICC'17, PIMRC'17, and VTC-Spring'18 conferences. His research interests involve signal processing with applications to communications and navigation based on satellite and terrestrial technologies.



Universitat Autònoma de Barcelona, Barcelona, Spain, where he has also been Vice Dean of the Engineering School since 2011 and he is currently a Professor. His research interests include satellite and terrestrial localization systems. Since 2018, he has been serving as a member of the Sensor Array and Multichannel Technical Committee of the IEEE Signal Processing Society. He was a recipient of the 2013 ICREA Academia Award.



Massachusetts Institute of Technology from 2018 to 2019. He is an Associate Editor of IEEE TRANSACTIONS ON VEHICULAR TECHNOLOGY. His research interests include wireless communications/positioning/localization, signal processing, vehicular networks, estimation/statistical inference, and machine learning.



appointments at the Coordinated Science Laboratory, University of Illinois Urbana-Champaign, the University of California Irvine, Hanyang University, and the European Commission Joint Research Center. His research interests lie in the field of signal processing for communications and navigation, with special emphasis on cloud GNSS signal processing and the convergence between GNSS and 5G terrestrial cellular networks. He is the Secretary and Treasurer of the Spain Chapter of the IEEE Aerospace and Electronic Systems Society.

José A. del Peral-Rosado (S'12–M'15) received the Ph.D. degree in telecommunications engineering from Universitat Autònoma de Barcelona (UAB), Bellaterra, Spain, in 2014. Since 2014, he has been a Postdoctoral Researcher with the Department of Telecommunications and Systems Engineering at UAB. From 2014 to 2016, he was a Visiting Researcher at the European Space Research and Technology Centre (ESTEC) of the European Space Agency (ESA) under the NPI programme. He is actively involved in COST CA15104 (IRACON), and he gave tutorials at IEEE ICC'17, PIMRC'17, and VTC-Spring'18 conferences. His research interests involve signal processing with applications to communications and navigation based on satellite and terrestrial technologies.

Gonzalo Seco-Granados (S'97–M'02–SM'08) received the Ph.D. degree in telecommunications engineering from Universitat Politècnica de Catalunya, Barcelona, Spain, in 2000, and the M.B.A. degree from the IESE Business School, Barcelona, Spain, in 2002. From 2002 to 2005, he was a member of the European Space Agency, where he was involved in the design of the Galileo System. In 2015, he was a Fulbright Visiting Professor with the University of California at Irvine, Irvine, CA, USA. Since 2006, he has been with the Department of Telecommunications, Universitat Autònoma de Barcelona, Barcelona, Spain, where he has also been Vice Dean of the Engineering School since 2011 and he is currently a Professor. His research interests include satellite and terrestrial localization systems. Since 2018, he has been serving as a member of the Sensor Array and Multichannel Technical Committee of the IEEE Signal Processing Society. He was a recipient of the 2013 ICREA Academia Award.

Sunwoo Kim (S'99–M'05–SM'17) received the B.S. degree from Hanyang University, Seoul, Korea in 1999, and the Ph.D. degree, in 2005, from the University of California, Santa Barbara, CA, USA. Since 2005, he has been with the Department of Electronic Engineering at Hanyang University, Seoul, South Korea, where he is currently a Professor. He is also the Director of the 5G/Unmanned Vehicle Research Center, funded by the Ministry of Science and ICT of Korea, and now a Visiting Scholar at Laboratory for Information and Decision Systems,

José A. López-Salcedo (M'10–SM'16) received the Ph.D. degree in telecommunication engineering from Universitat Politècnica de Catalunya (UPC), Barcelona, Spain, in 2007. In 2006, he joined the Department of Telecommunication and Systems Engineering, Universitat Autònoma de Barcelona (UAB), where he is an Associate Professor. He has been the Principal Investigator of more than 15 research projects, most of them funded by the European Space Agency (ESA) on topics dealing with signal processing for GNSS receivers. He has held several visiting